

Article

Antibacterial Effect of Polymethyl Methacrylate Resin Base Containing TiO₂ Nanoparticles

Anamarija Zore ¹, Anže Abram ², Aleksander Učakar ², Ivo Godina ¹, Franc Rojko ¹, Roman Štukelj ¹, Andrijana Sever Škapin ^{3,4}, Rajko Vidrih ⁵, Olivera Dolic ⁶, Valentina Veselinovic ⁶ and Klemen Bohinc ^{1,*}

¹ Faculty of Health Sciences, University of Ljubljana, 1000 Ljubljana, Slovenia

² Jožef Stefan Institute, 1000 Ljubljana, Slovenia

³ Slovenian National Building and Civil Engineering Institute, 1000 Ljubljana, Slovenia

⁴ Faculty of Polymer Technology—FTPO, Ozare 19, 2380 Slovenj Gradec, Slovenia

⁵ Biotechnical Faculty, University of Ljubljana, 1000 Ljubljana, Slovenia

⁶ Faculty of Medicine, University of Banja Luka, 78000 Banja Luka, Bosnia and Herzegovina

* Correspondence: klemen.bohinc@zf.uni-lj.si

Abstract: Restorations in dentistry must reproduce the aspect of the patient's natural teeth and require non-toxicity, biocompatibility, and good mechanical properties in order to last longer. Restorations are permanently in contact with microbes that can adhere to and form biofilms. The purpose of this study was to determine the adhesion extent of *Streptococcus mutans* to polymethyl methacrylate (PMMA) resin base containing TiO₂ nanoparticles. To understand the adhesion of *Streptococcus mutans* on the modified resin-based surfaces, the following surface properties were measured: the roughness, contact angle, zeta potential and CIE color parameters. Evaluation of tensile stress performance in TiO₂ modified PMMA showed that the maximum tensile stress of the modified PMMA resin decreases with an increasing amount of TiO₂ nanoparticles. The increasing amount of TiO₂ decreases the roughness and causes contact angles in the border between hydrophilic and hydrophobic surfaces. All the studied surfaces are negatively charged and added TiO₂ tends to increase the zeta potential. The addition of TiO₂ nanoparticles increases the lightness and decreases the intensity of the red and yellow color. The increasing addition of TiO₂ nanoparticles into PMMA increases the morphological change of bacterial cells.

Keywords: bacterial adhesion; *Streptococcus mutans*; polymethyl methacrylate resin; TiO₂; surface properties



Citation: Zore, A.; Abram, A.; Učakar, A.; Godina, I.; Rojko, F.; Štukelj, R.; Škapin, A.S.; Vidrih, R.; Dolic, O.; Veselinovic, V.; et al. Antibacterial Effect of Polymethyl Methacrylate Resin Base Containing TiO₂ Nanoparticles. *Coatings* **2022**, *12*, 1757. <https://doi.org/10.3390/coatings12111757>

Academic Editor: James Kit-Hon Tsoi

Received: 8 September 2022

Accepted: 26 October 2022

Published: 16 November 2022

Publisher's Note: MDPI stays neutral with regard to jurisdictional claims in published maps and institutional affiliations.



Copyright: © 2022 by the authors. Licensee MDPI, Basel, Switzerland. This article is an open access article distributed under the terms and conditions of the Creative Commons Attribution (CC BY) license (<https://creativecommons.org/licenses/by/4.0/>).

1. Introduction

As a consequence of the general aging of human population, an increasing number of totally or partially toothless patients are being registered. As a consequence of the general aging of human population, an increasing number of totally or partially toothless patients are being registered. Observed at the global level, the number of elderly people tends to grow and, according to United Nations data, by 2050 the percentage of elderly people will be 16% (UN2019) [1]. The prevalence of tooth loss gradually increased with age, with a peak in incidence at 65 years [2]. Despite the development of implant prosthetics and the availability of implants in clinical practice, a significant number of people, due to lack of material resources, can still afford only the option of total or partial dentures. This type of prosthetic reconstruction involves gingival-supported restoration with a large area of support on the soft tissues of the oral cavity. Polymethyl methacrylate is the most commonly used denture base material in dental practice [3]. These resins commonly consist of methyl methacrylate (MMA) and polymethyl methacrylate (PMMA) [4].

This polymer is the material of choice for fabrication of denture base due to its good properties such as proven high degree of biocompatibility, simple prosthesis production technology, low density, low weight, ease of finishing and polishing, stability in oral

environment, satisfactory aesthetics, color matching ability, reparability, reasonable price and relatively satisfactory physical and mechanical properties [5,6]. Although this material has been used for many years in practice, some limitations of this material, such as limited mechanical resistance against fatigue, impact and flexural strengths, conductivity, water sorption, solubility and insufficient surface hardness are still the subject of numerous studies [7–9].

Recently, numerous studies have been conducted in the field of incorporation of inorganic nanoparticles into PMMA in order to improve their properties. For example, several studies reported the improvement of PMMA materials modified with addition of variety of fibers, nanoparticles and nanotubes [10–12]. These nanocomposites are conventional polymethylmethacrylates modified by the addition of a low percentage of nanoparticles in the range between 1 nm and 100 nm, in order to change their properties [6].

In addition to the concentration of nanoparticles, their shape and size, as well as the interaction with the polymer matrix determine the new properties of nanocomposites [13]. Nanoparticles are known for their superior performance over conventional particle sizes of its materials. When nanoparticles are incorporated into a polymeric matrix as fillers, the characteristics of both ingredients are integrated to improve the optical, mechanical and biological properties of the nanocomposites [14].

The most significant disadvantage of denture base PMMA material, observed from the clinical aspect, is the susceptibility to plaque accumulation on the gingival surface of the prosthesis. Surface roughness, porosity, continuous wearing of dentures as well as poor hygiene can lead to colonization of the denture surface by microorganisms and the formation of a resistant microbial biofilm [15–17]. Microbial biofilm on the prosthesis surface is a source of infection and in the complete prosthesis wearer can lead to the development of prosthetic stomatitis, which affects the prosthesis supporting gingival soft tissues. Virulent microorganisms can be separated from the developed biofilm on the prosthesis base, and in old, immunocompromised patients, they can cause opportunistic infections with the development of aspiration pneumonia [18,19]. Extensive and inadequately indicated use of antibiotics has led to the development of drug resistance of many bacterial and fungal species, which is an aggravating factor in conventional therapy.

Modern studies have evaluated various approaches in improving the reduction of infection risk in total denture wearers, among which the researchers' special attention was drawn to the modification of conventional acrylates to make a denture base by adding different nanoparticles (NPs)—TiO₂, SiO₂, ZnO, CuO, ZrO₂, Ag and similar [20–24].

Among these nanoparticles, TiO₂ nanoparticles stood out due to their high stability, photocatalytic effect, non-toxicity, high refractive index, corrosion resistance, high hardness, potential antimicrobial activity, availability and affordable price [25–27]. The addition of TiO₂ nanoparticles to the polymer matrix, even in very small percentages, affects the electrical, optical, chemical and physical properties of the material [25]. Previous studies have shown that, due to their photocatalytic activity, TiO₂ nanoparticles show antimicrobial activity against a wide range of gram-positive, gram-negative bacteria, fungi and viruses [21,25,26,28]. The antimicrobial activity of TiO₂ nanoparticles may be associated with nanoparticle surface and structure properties such as TiO₂ nanocrystalline structure, surface hydrophilicity, infrared reflectivity, and non-contact antimicrobial activity [25–31].

Factors that contribute to the adhesion of microorganisms to acrylic resins and the subsequent formation of biofilm are the surface roughness, charge, wettability, porosity, continuous wearing of dentures and poor hygiene of dentures [32–34]. Additionally, specific surface contours of the gingival surface of the prosthesis and the oral mucosa enhance the microbial adhesion [35]. In order to better understand the microbial adhesion, the surfaces need to be characterized.

The insertion of TiO₂ nanoparticles into the polymer matrix is part of a modern approach to the development of denture bases with antimicrobial potential [30]. Results of previous studies have shown that modification of the prosthesis PMMA base with the

addition of TiO₂ NPs improves the antimicrobial properties of the material, reducing the formation of microbial biofilm [36–39].

Some scientific studies have proven the antimicrobial activity of TiO₂ nanoparticles for other medical purposes [39]. Also, some other authors reported that as the ratio of TiO₂ to PMMA-TiO₂ increases, the antimicrobial properties of PMMA drastically reduce bacterial adhesion [37,38]. Chen and coauthors reported that 3 wt% additions of various antibacterial agents, including TiO₂ NPs based agents, had significantly antibacterial activities compared to the control and blank groups ($p < 0.05$). The antibacterial rate of 3% additions of TiO₂, Ag/TiO₂, Novaron, T-ZnO antibacterial agents are 30.26, 67.82, 61.69 and 49.81% against *S. mutans* [30]. Silicon / titanium nanoparticles in dental prostheses significantly reduce microbial adhesion [26]. One of the main advantages of TiO₂ NP is their ability to use at least two different mechanisms of antimicrobial action, so the probability of developing resistance to TiO₂ NP is very low [40].

Color of restoration materials must match as close as possible the color of human gingiva. Color is often expressed in L*a*b* CIELAB color space. It expresses color in three coordinates: L* stands for lightness (100 = light; 0 = dark), a* stands for red/green (positive values = red; negative values = green) while b* stands for yellow /blue (positive values = yellow; negative values = blue). In average, human gingiva has the following color coordinates: L* = 52.9, a* = 23.3 and b* = 14.9 [41]. Exact values of color parameters depend on age, ethnicity and gender [41].

There is a lack of knowledge and understanding in the modern literature regarding the effectiveness of these fillers and their optimal concentrations in the denture base material. The existing study evaluates the influence of different concentrations of TiO₂ nanoparticles (TiO₂ NPs), incorporated in heat-polymerized PMMA for prosthesis base, on the mechanical, aesthetic and antimicrobial properties of this material.

The expansive development of nanomaterials and nanotechnologies has led to numerous research efforts to overcome the shortcomings of conventional acrylates in dentistry, as well as to improve their existing good properties. The addition of organic and inorganic nanoparticles to the polymer matrix to improve the physical, mechanical and antimicrobial properties of PMMA is currently a very actual direction in research. The addition of inorganic nanoparticles such as metals and metal oxides has received more attention due to their ability to withstand more severe conditions such as those registered in the oral cavity [42].

2. Materials and Methods

2.1. Materials

2.1.1. Bacteria

In this study, *Streptococcus mutans* (*S. mutans*) ATCC 25175 standard strains were used and selected from the culture on blood-agar plates incubated at 37 °C for 48 h with a CO₂ pack (Gas-pak method) for anaerobic conditions. The *S. mutans* overnight culture was prepared in BHI (brain-heart infusion) nutrient broth (Biolife, Italiana Srl) (4012302) at 37 °C for 18 h to obtain 10⁹ CFU mL⁻¹ of bacterial suspension. The overnight culture was diluted at 1:30 in fresh BHI medium to obtain proximal 10⁸ CFU mL⁻¹. Samples of PMMA with different amounts of added TiO₂ were incubated for 10 h at 37 °C in five milliliters of bacterial suspension with a cell concentration of 10⁸ CFU mL⁻¹ [43]. After 10 h of incubation, the PMMA samples with attached bacteria were rinsed in PBS buffer and fixed with hot air. The PMMA samples with added TiO₂ with attached and fixed bacteria were examined with a scanning electron microscope.

2.1.2. PMMA/TiO₂ NPs

The monomer (powder) and polymer (liquid) are mixed and the mass is left on the pre-polymerization phase for 10 min. If nanoparticles are added, they are added at this stage. After 10 min, the prepared form of the test pieces is crushed, pressed in a pneumatic press (Shuler dental, Ulm, Germany) and then polymerized in the apparatus. The temperature

rise is 2.5 °C per minute (polymerization takes place at a temperature from 25 °C to 100 °C) and then stands for 35 min at 100 °C. After this time, the heater is turned off and the object is slowly cooled to room temperature, when the test piece is removed from the mold, treated with abrasives and polished.

PoliCOLD material was used, which is an acrylate for the manufacture of prostheses. For elastic measurements, the PMMA resins were prepared in dimensions of 15 mm × 80 mm and with a thickness of 3 mm. The PMMA resins were prepared in the dimension of 1 cm × 1 cm and a thickness of 2–3 mm and for zeta potential measurements in the dimension of 1 cm × 2 cm. For the preparation of three 1 cm × 1 cm and two 1 cm × 2 cm samples, 11 g of heat-curing polymerizing acrylate powder and 5 mL of binding fluid was used. In the case of 1% added TiO₂ 0.11 g of TiO₂ powder was added, and for 5% added TiO₂ 0.5 g of TiO₂ powder was added. An amount of 10% and 20% added TiO₂ was prepared only in the terminating layer (very thin film on one side). A 10% addition of TiO₂ in the terminating layer was performed by 3 g of polymerizing acrylate powder, 1.3 mL of binding fluid and 0.3 g of TiO₂ powder. A 20% addition of TiO₂ in the terminating layer was obtained by 3 g of polymerizing acrylate powder, 1.3 mL of binding fluid and 0.6 g powder of TiO₂.

Titanium (IV) oxide powder was purchased from Sigma Aldrich (armstadt, Germany). The primary particle size (TEM) is 21 nm. CAS Number: 718467-100G.

The artificial tooth is made of composite. Artificial teeth are part of the total prostheses and were included in this study in order to make a comparison with PMMA.

2.2. Methods

2.2.1. Mechanical Properties of PMMA with and without TiO₂ Added

The uniaxial tensile tests of the selected materials were performed using Z030 apparatus (Zwick, Ulm, Germany) at a temperature of 23 °C and a relative humidity of 50%. The testing speed was 2 mm/min. For each group of material, three to five measurements were performed. Prior testing specimens were conditioned for 3 days at 23 °C and 50% relative humidity. A preloading of 10 N was used. The starting distance between the grips and the initial gauge length was 50 mm and 20 mm, respectively.

To measure the tensile strength of PMMA, test pieces in the dimension of 80 mm × 15 mm × 2.5 mm for each type were prepared.

2.2.2. Roughness Measurements

The PMMA surface topographies were measured and characterized by profilometer Form Talysurf Series 2 (Taylor-Hobson Ltd., Leicester, UK). The resolution was of 0.25 μm, 1 μm and 3 nm in the x, y and z directions, respectively. A set of parallel line scans was performed with a tip of 2 μm.

Data were processed using TalyMap Gold 6.2, and the quantitative evaluation of surface features was achieved. Using the statistical analysis, the roughness parameters were calculated. To separate roughness from waviness, a Gaussian cut-off filter of 0.8 mm was used. On each type of PMMA surface, three-line measurements in the length of 5 mm were made. From the data, the analysis of the roughness was made, and the arithmetic average roughness (R_a) and root mean square roughness (R_q) were calculated.

2.2.3. Contact Angle Measurements

Contact angle measurements were performed by the Attension Theta (Biolin Scientific, Gothenburg, Sweden) tensiometer. The equipment consists of a light source, camera, liquid dispenser and a sample stage. PMMA surfaces were placed on the sample stage and a liquid droplet of deionized water was placed on the PMMA surface. The contact angle between the droplet and the surface was measured. The angle was measured in an time interval of 10 s with frame rate of 3.3 FPS. For each measurement the average contact angle was calculated between 1–9 s. Eight measurements were made for each material and the average value of the contact angle with standard error was obtained.

2.2.4. Zeta Potential Measurements

The zeta potential of PMMA surfaces was measured by an electro-kinetic analyzer (SurPASS, Anton Paar GmbH, Graz, Austria) containing a disk-adjustable gap cell. Two PMMA surfaces were fit into the cell facing each other in parallel with a micro split of 100 μm . An amount of 1 mM of phosphate-buffered saline (PBS) solution was forced to flow through the capillary at room temperature and pH = 7.4. The electrostatic potential was produced between the ends of the capillary. Using the Smoluchowski equation, the measured potential was converted to the zeta potential ζ .

2.2.5. Color Measurements

The color of PMMA resins with TiO_2 addition was measured with a colorimeter (CR-400; Minolta, Kyoto, Japan) in CIELAB color space referred to as $L^*a^*b^*$. The data were analyzed according to the Commission Internationale de l'Éclairage (CIE). The total color difference (ΔE) was calculated as given in equation $\Delta E = ([\Delta a^*]^2 + [\Delta b^*]^2 + [\Delta L^*]^2)^{1/2}$, with ΔE classified as 'very distinct' for $\Delta E > 3$, 'distinct' for $1.5 < \Delta E < 3$, and 'nondistinct' for $\Delta E < 1.5$.

2.2.6. Bacterial Rate Measurement, SEM Micrographs and EDS Analysis

After 10 h of incubation the PMMA samples with attached bacteria were rinsed in PBS buffer and fixed with hot air. PMMA samples with added TiO_2 with attached and fixed bacteria were examined with a scanning electron microscope (SEM, Quanta 650, Thermo Fisher Scientific, Waltham, Massachusetts, United States). The samples were coated with gold (BAL-TEC SCD 005, BALTEC AG, Pfäffikon, Switzerland) and the thickness of the gold layer was ~ 5 nm. The vacuum during gold coating was 5×10^{-2} . The working distance of 10 mm at the accelerating voltage of 10 kV and vacuum 2×10^{-4} was used for imaging by the secondary electron sensor.

The EDS elemental analysis (Ultim Max SDD 40 mm², Oxford Instruments, Abingdon, United Kingdom) was performed at 30 kV and WD = 10 mm at low magnification in order to include the most relevant features.

The quantitative analysis of the bacterial coverage on SEM micrographs was obtained by manually encircling the bacteria and converting the images to the binary form. We used the ImageJ software package (Version 1.50b, 2015, Wayne Rasband, National Institutes of Health, Bethesda, MD, USA) for further analysis; 23 micrographs, representing a total area of 38,000 μm^2 , were analyzed to determine the coverage of *S. mutans* on the substrates.

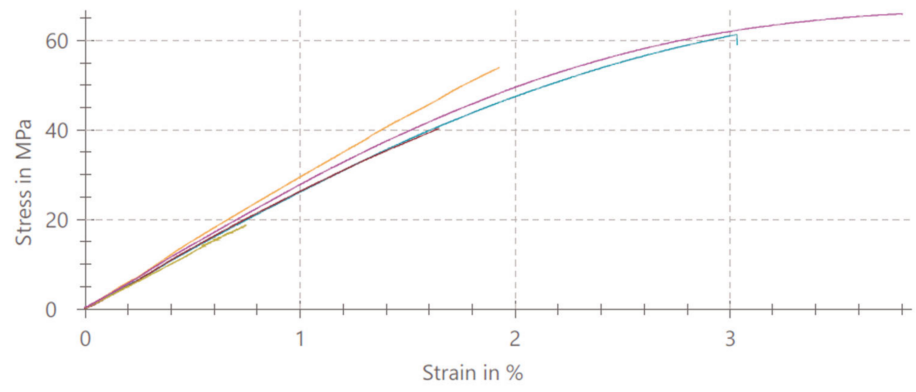
3. Results

3.1. Mechanical Properties of PMMA/ TiO_2 NPs

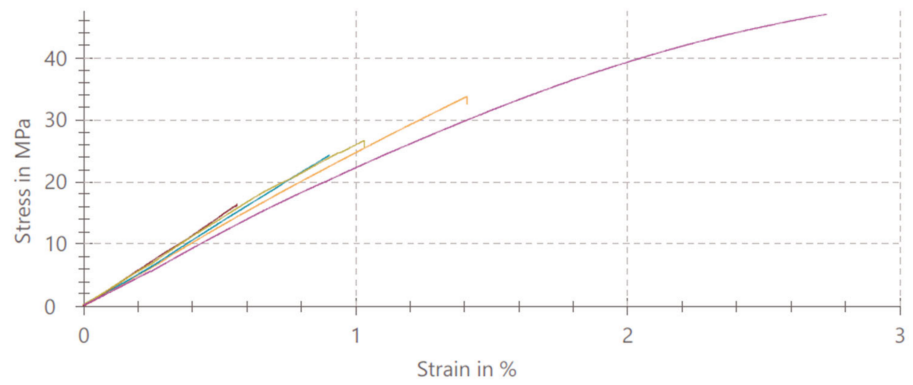
The stress–strain curves of the tensile test for samples, PMMA, PMMA/ TiO_2 NPs (1%) and PMMA/ TiO_2 NPs (5%), PMMA/ TiO_2 NPs (10%), and PMMA/ TiO_2 NPs (20%) are presented in Figure 1.

The mean values and standard deviations of three to five measurements of the maximum tensile stress (σ_M) and the corresponding strain (ε_M) are shown in Table 1. For all measurements, σ_M and ε_M were found at the end of the curves, at the break that occurred. PMMA without additive has the highest value of σ_M (48.1 MPa) at ε_M 2.2%. The maximum tensile stress was reduced by increasing the quantity of TiO_2 incorporation in PMMA. In the case of PMMA/ TiO_2 NPs (1%), σ_M and ε_M are 29.6 MPa and 1.3%, respectively. For PMMA/ TiO_2 NPs (5%), σ_M and ε_M are 22.7 MPa and 1.0%, respectively, while for the two samples with the largest incorporation of TiO_2 , 10% and 20% of the tensile stress is 22.2 MPa and 21.7 MPa at ε_M 1.9% and 2.5%, respectively. All the measured properties have relatively large standard deviations.

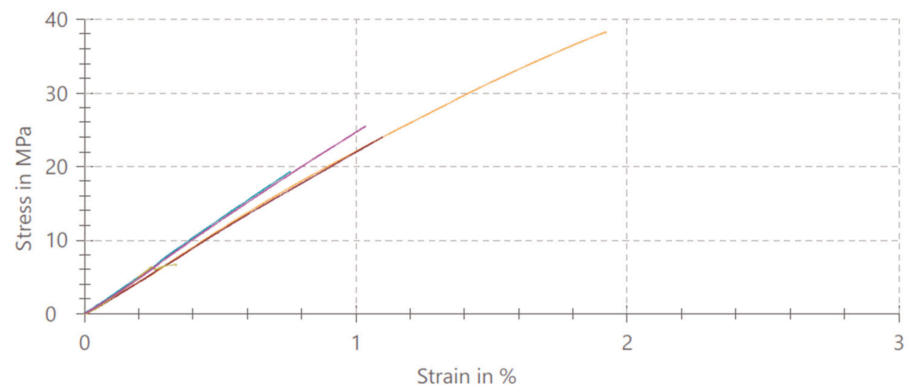
We observe that in the case of PMMA/ TiO_2 NPs (10%) and PMMA/ TiO_2 NPs (20%) we reduce the decrease in the maximum tensile stress.



(a)



(b)



(c)

Figure 1. Cont.

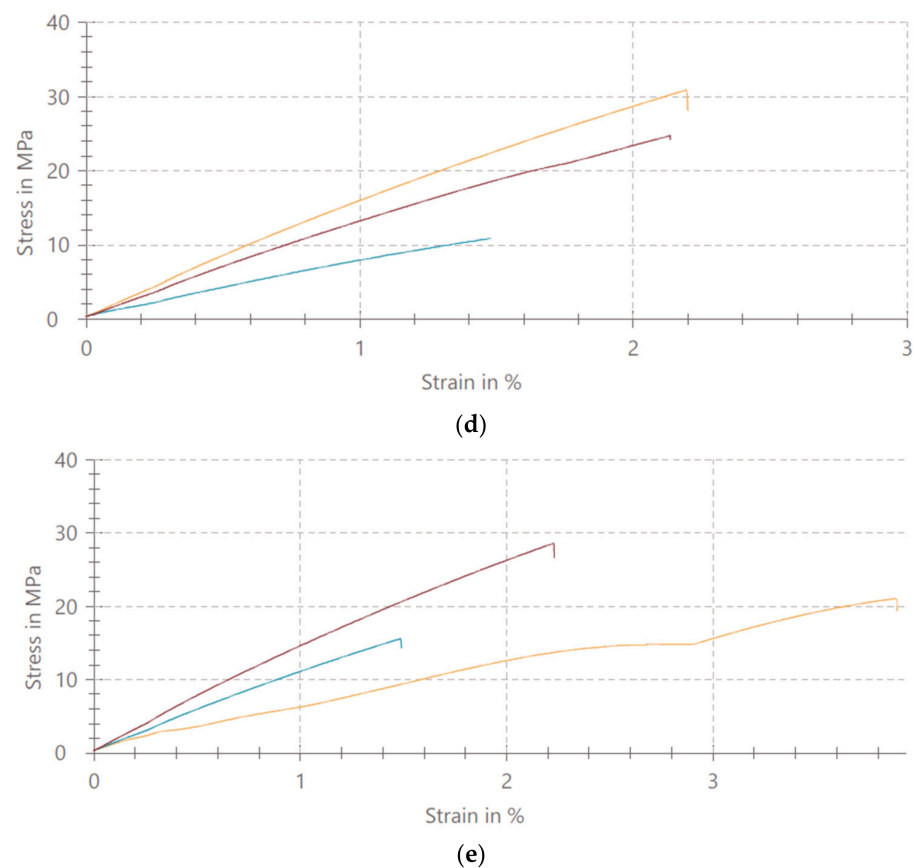


Figure 1. The stress–strain curves of tensile test for (a) PMMA, (b) PMMA/TiO₂ NPs (1%), (c) PMMA/TiO₂ NPs (5%), (d) PMMA/TiO₂ NPs (10%) and (e) PMMA/TiO₂ NPs (20%).

Table 1. The mean values with standard deviations of the maximum tensile stress (σ_M) and the corresponding strain (ϵ_M) of PMMA samples.

	σ_M (MPa)	ϵ_M (%)
PMMA	48.1 ± 19.0	2.2 ± 1.2
PMMA/TiO ₂ NPs (1%)	29.6 ± 11.5	1.3 ± 0.8
PMMA/TiO ₂ NPs (5%)	22.7 ± 11.4	1.0 ± 0.6
PMMA/TiO ₂ NPs (10%)	22.2 ± 10.3	1.9 ± 0.4
PMMA/TiO ₂ NPs (20%)	21.7 ± 6.5	2.5 ± 1.2

3.2. Roughness

The roughness of PMMA/TiO₂ NPs surfaces was measured using the profilometer with a stylus that runs on the surface of a sample. From the profilometer's data the arithmetic average roughness R_a was calculated and presented for all six types of surfaces, as shown in Figure 2. The highest roughness was obtained for PMMA with 1% of TiO₂, $R_a = (0.93 \pm 0.2) \mu\text{m}$. The roughness of PMMA with 20% added TiO₂ was $R_a = (0.35 \pm 0.02) \mu\text{m}$. The lowest roughness was measured on the artificial teeth.

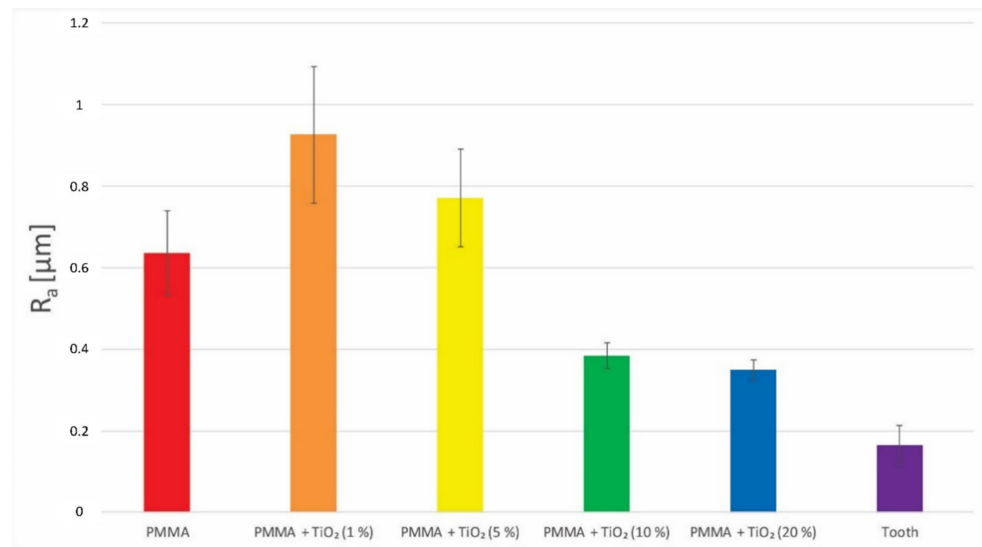


Figure 2. Arithmetic average roughness R_a of surfaces measured with profilometer.

3.3. Contact Angle

The hydrophobicity of PMMA surfaces is described by the contact angle measurements. Figure 3 shows the contact angles of the liquid droplet on the surface of all five material surfaces and the artificial tooth. The highest contact angle was measured for PMMA with 1% added TiO₂. For a higher amount of added TiO₂, the contact angle lies between 80° and 90°, which indicated that the surfaces are weakly hydrophilic.

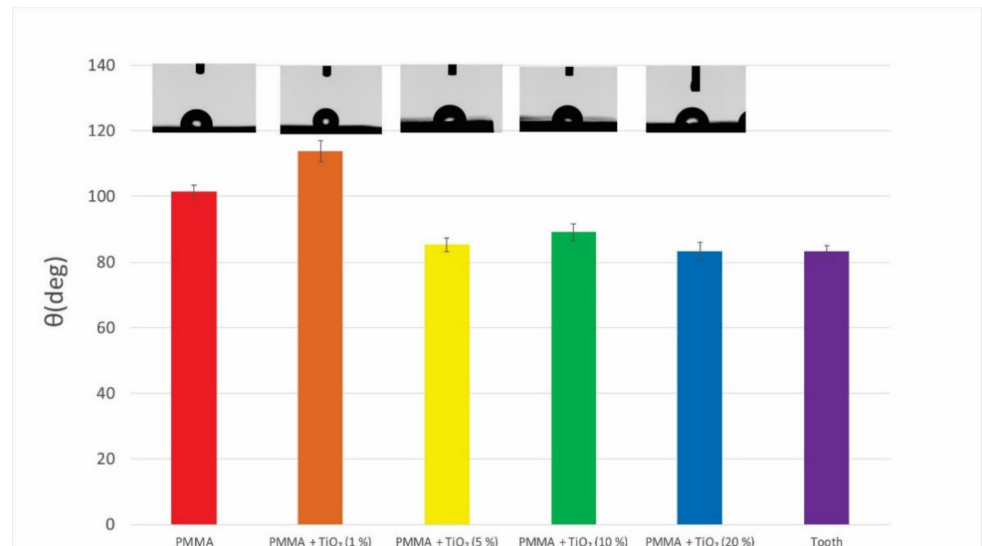


Figure 3. Contact angles of all five PMMA/TiO₂ NPs surfaces measured by the tensiometer. In inset the pictures of water droplets on the surfaces are shown.

3.4. Zeta Potential

Figure 4 shows the zeta potentials of five PMMA surfaces measured at room temperature and pH = 7.4. The results show that all materials are negatively charged. The absolute values of the zeta potential are very similar and close to −30 mV. Due to the geometrical restrictions, the zeta potential of the artificial tooth was not possible to measure.

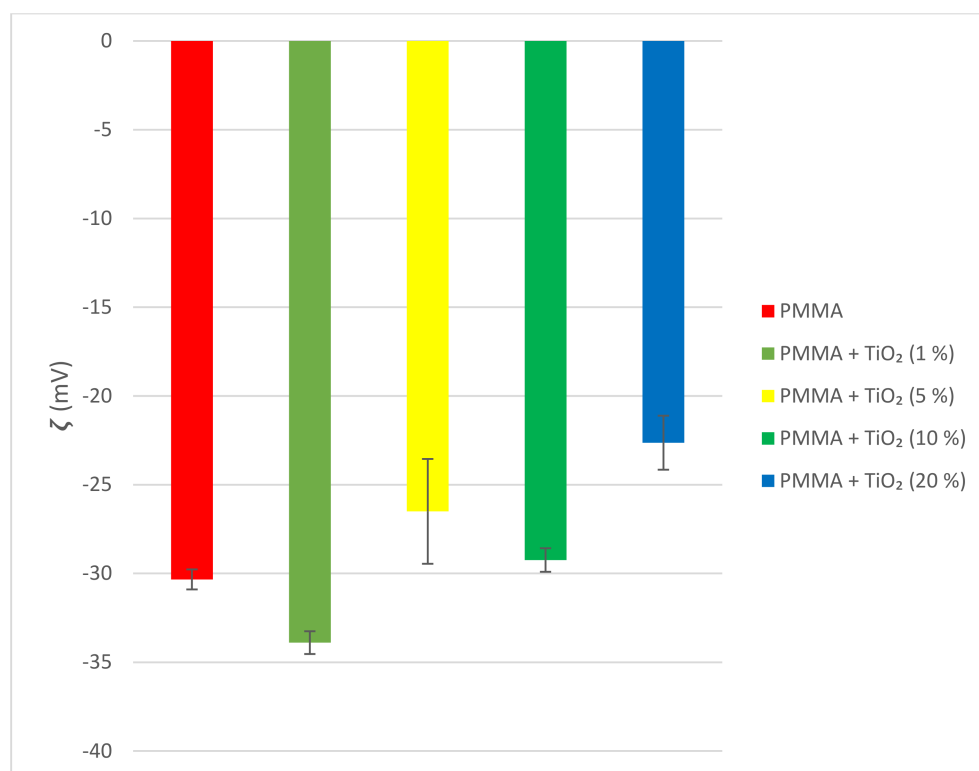


Figure 4. Zeta potentials of all PMMA/TiO₂ NPs surfaces.

3.5. Color Parameters

As seen from Table 2, the PMMA material has an intermediate L* value within the 50–100 range, which is represented by a red color (positive a* value) and a yellow color (positive b* value). Increasing the TiO₂ content (0–20%) results in a lighter color, as evidenced by an increased L* value (57.6–85.0). The intensity of the red color decreased from 22.2 to 6.1 with an increasing content of TiO₂. Similarly, the intensity of the yellow color decreased from 14.4 to 2.7 with an increasing content of TiO₂. The addition of TiO₂ thus increased the lightness and decreased the intensity of the red and yellow color.

Table 2. CIE L*, a*, b* color parameters of PMMA and its TiO₂ derivations.

	L*	a*	b*	ΔE
PMMA	57.6 ± 0.38	22.2 ± 0.42	14.4 ± 0.22	4.85
PMMA + TiO ₂ (1%)	72.0 ± 0.44	16.7 ± 0.26	8.4 ± 0.43	21.23
PMMA + TiO ₂ (5%)	78.9 ± 0.37	14.1 ± 0.44	5.9 ± 0.37	29.01
PMMA + TiO ₂ (10%)	81.3 ± 0.28	7.8 ± 0.87	3.4 ± 0.44	34.34
PMMA + TiO ₂ (20%)	85.0 ± 0.29	6.1 ± 0.22	2.7 ± 0.10	38.41

As seen in Table 2, the total color difference ΔE expresses the difference between the PMMA derivations and gingiva color, as reported by Ho et al. 2015 [30]. It is evident that basic PMMA with no TiO₂ already shows discoloration, while increasing TiO₂ addition results in an increased ΔE amounting to 38.41 for PMMA + 20% TiO₂.

Waldemarin et al. (2013) tested three polymerization techniques, i.e., microwave irradiation/microwave-activated resin, heat polymerization/conventional heat-activated resin and microwave irradiation/conventional heat-polymerized resin. The immersion of resins in the tested beverages (water, cola, coffee, mate tea and red wine) changed the color of the resins in ascending order. The highest ΔE changes were observed for a combination of coffee-microwave irradiation/conventional heat-polymerized resin. In an accelerated ageing experiment (200 h of UV irradiation, thermocycling) of acrylic resin and

nylon-based polymer dentures, Hamed et al. (2017) reported more noticeable chromatic changes of acrylic resin as compared to nylon-based polymers. Comparing nanoparticles or fiber-reinforced PMMA, Alhotan et al. (2022) found the color of TiO₂-reinforced PMMA to be the least stable as compared to ZrO₂ or fiber-reinforced.

3.6. Bacterial Adhesion Rate Measurement, SEM Micrographs, EDS

Figure 5 shows the SEM micrographs of PMMA/TiO₂ NPs surfaces with adhered *S. mutans*. The results of the bacterial adhesion extent of *S. mutans* on five materials show that the addition of TiO₂ increases the morphological change of bacterial cells. For pure PMMA, the surface coverage of a single bacterium is 73%. An amount of 1% and 5% added TiO₂ decreases the single surface coverage to 18.8% and 44.9%, respectively. Up to an amount of 1% added TiO₂ do not causes morphological change of adhered bacterial cell, whereas 5% added TiO₂ causes 33.4% morphological change of adhered bacterial cells, respectively. An amount of 10% of added TiO₂ decreases the single bacterial extent to 12%, whereas 20% of added TiO₂ decreases the single bacterial adhesion extent to 23%. In the last two cases (10% and 20% of added TiO₂), the morphological change starts to become important. A total of 58% (10% added TiO₂) and 60% (20% added TiO₂) of the bacterial cells are covered with extracellular polymeric substances (EPS). The artificial tooth has a coverage of bacteria lower than 25%.

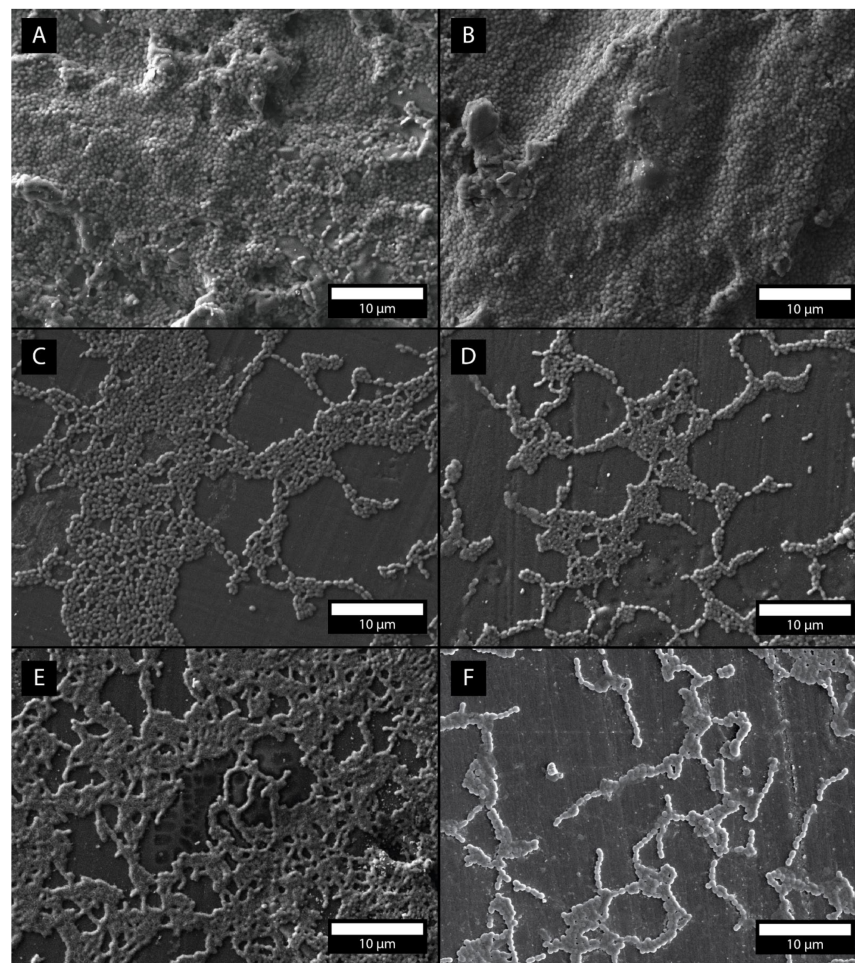


Figure 5. SEM micrographs with adhered bacteria *S. mutans* for all five PMMA surfaces. (A) 0%, (B) 1%, (C) 5%, (D) 10% and (E) 20% of TiO₂ added. (F) Artificial tooth.

The elemental analysis shows that with the higher concentration of added TiO₂ NPs the aggregation of NPs takes place (Figure 6).

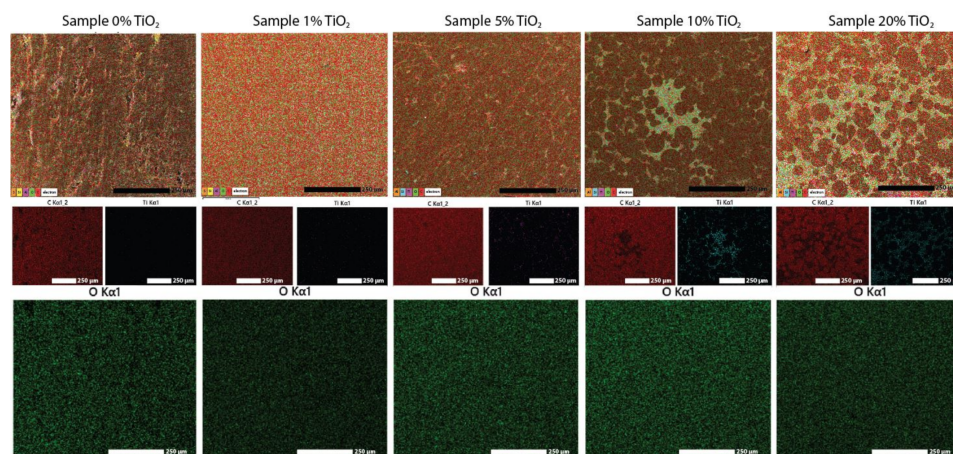


Figure 6. The presence of elements in the samples by EDS analysis. The images correspond to 0%, 1%, 5%, 10% and 20% of added TiO_2 into PMMA. First colon shows the distribution of the following elements: orange—S, yellow—Si, purple—Al, green—O and red—C. Second colon corresponds only to C and Ti.

EDS was performed on carbon-sputtered samples on a working distance of 10 mm with an open detection in order to observe all possible elements. EDS mapping was performed to check the distribution of TiO_2 NP. Some artefacts on the sample can cause the additional presence of C and/or O. Additionally, any cracks and edges can produce a shadow that is seen on all elemental maps and observed as a lower contrast, indicating a material change which is not real. The EDS analysis shows that the agglomeration of nanoparticles into micron clusters is present. This can significantly affect the mechanical properties of the composite due to the notch effect.

4. Discussion

The objectives of this study were to evaluate the effects of TiO_2 nanoparticles (in concentrations of 1%, 5%, 10% and 20%) on the uniaxial tensile strength, the color change of TiO_2 NPs-modified PMMA denture base material, surface properties as zeta potential, roughness and contact angle, and on the formation of *S. mutans* biofilm on the denture surface of PMMA/ TiO_2 NPs.

4.1. Mechanical Properties of PMMA/ TiO_2 NPs

The tensile test results of PMMA/ TiO_2 NPs show that the tensile strength decreases with an increasing concentration of TiO_2 NPs (Table 1).

Examining the tensile strength of PMMA with 0.5%, 1% and 5% TiO_2 NPs, Shirkavand and Moshlehifard concluded that the tensile strength increases with an increasing concentration of TiO_2 NPs to 1 wt%, showing an improvement in the tensile strength of 35% compared to pure PMMA, and then decreases with an increase in TiO_2 NPs concentration of 5% due to the formation of TiO_2 NPs clusters [44]. The possible reasons for this could be the improper dispersion of TiO_2 and the formation of agglomerates in the PMMA matrix, and consequently, a higher amount of unreacted monomer, which acts as a plasticizer [45]. Previous studies have shown that an increase in the concentration of TiO_2 NPs leads to the appearance of a larger number of agglomerates. The reason for the formation of conglomerates can be found in the van der Waals forces between TiO_2 NPs, which make dispersion in polymethyl methacrylate difficult [46].

Agglomerates act as the centers of stress concentration within the matrix and negatively affect the mechanical properties of the polymerized material. Preventing agglomeration in material production technology is one of the main challenges in nanocomposite production. The concentration of stress in the area of formed agglomerates probably leads to the formation of micro-pores and micro-cracks. These defects were not present in the low percentages of TiO_2 NPs. Larger accumulations of TiO_2 NPs in the PMMA matrix act

as an impurity of the polymer matrix and negatively affect the mechanical properties of the material [44,47].

According to a study by Ghaheremani et al. (2017), PMMA with 1% TiO₂ NPs shows significantly higher tensile strength compared to conventional unmodified acrylate, which they attribute to the fact that the applied force is mostly tolerated over added NP [48]. Contrary, Chatterjee found an increase in the tensile strength of up to 95% by incorporating higher concentrations of TiO₂ NPs (5% and 15%) in PMMA. They considered that this result was caused by strong adhesion between TiO₂ NPs and PMMA, where the applied force is transmitted through the intermediate phase of the surface to the strongest material, which are NPs [43].

With the increasing content of TiO₂ NPs, an increase in the number of micro-cracks in the structure of PMMA is observed. Alrahlaha et al. state that a smaller number of cracks was observed in PMMA samples with 1% TiO₂ NPs compared to samples containing 5% TiO₂ NPs [26].

It can be concluded that it is necessary to establish a protocol that improves the distribution of unclustered TiO₂ NPs in the PMMA matrix [44]. Increasing the concentration of TiO₂ can lead to the overload of the matrix with filler above the saturation point. The resin cannot include more filler particles, which leads to the saturation of material, the disruption of the material structure, and a negative impact on mechanical properties [44,49].

It was observed that the higher concentration of added TiO₂ NPs leads to stronger aggregation of NPs (Figure 6). This explains the decreasing σ_M and ϵ_M .

4.2. Surface Roughness

The surface roughness of PMMA/TiO₂ NPs depends on the concentration of added NPs. The surface roughness of PMMA with 1% of TiO₂ NPs is higher compared to pure PMMA. A total of 5% of added TiO₂ NPs decreases the surface roughness, but it is still higher than the surface of pure PMMA. In a series, the surface roughness decreases further with increasing TiO₂ NPs concentrations. A total of 10% of added TiO₂ NPs shows the lowest roughness.

Alwan and Alameer demonstrated an increase in the surface roughness of PMMA samples with 3% added TiO₂ NPs, which was associated with the presence of NPs on the sample surface [28]. Gad et al. emphasized the importance of changing the surface roughness of PMMA by adding TiO₂ NPs [25].

Surface roughness is a very important parameter for the adhesion of bacteria to PMMA surfaces. Recently, it was shown that very smooth surfaces do not favor bacterial adhesion. On the contrary, very rough surfaces prefer adhesion [26,35,36,42]. Defects such as cracks and gaps [50–52] present favorable places for bacteria to adhere because they protect them from external interactions. This study confirms the previous studies, and consequently, the bacterial adhesion is larger on rougher surfaces (see Figure 5).

4.3. Contact Angle

Surfaces with contact angles smaller than 90° are called hydrophilic, whereas the surfaces with contact angles greater than 90° are named hydrophobic. It was found that most of our surfaces are hydrophilic. Pure PMMA and PMMA with 1% added TiO₂ are hydrophobic. The results of hydrophobicity follow the rule that the decreasing roughness of hydrophilic surfaces makes them even more hydrophilic.

The hydrophobicity has an important consequence for initial bacterial adhesion and, later, bacterial colonization of the surfaces. It was found that the highest bacterial adhesion extent was on hydrophobic surfaces. The following rule applies: the hydrophobic bacterial strains prefer to adhere to hydrophobic surfaces [37,53]. Hashem et al. wanted to establish the relationship between the contact angle (wetting) and the amount of TiO₂ NPs in the PMMA resin and found that the addition of 1 wt% TiO₂ NPs reduced surface wetting, while the addition of more fillers improved wetting. This finding confirms the effect of fillers on the surface of composite material compared to pure PMMA [54].

4.4. Zeta Potential

The PMMA/TiO₂ NPs surfaces used in this study are negatively charged with the zeta potentials between -34 mV and -22 mV. *S. mutans* is negatively charged, as are most bacteria [38]. Positively charged surfaces attract negatively charged bacteria, whereas negatively charge surfaces repel negatively charged surfaces. The zeta potential measurement indicates that the surfaces are highly negatively charged, which contributes roughly the same repulsive force between bacteria and all surfaces considered.

4.5. Color Parameters

The addition of TiO₂ gives PMMA a lighter color and less reddish and yellowish tones. The color parameters of basic PMMA material (L^* 52.9, b^* 23.3, b^* 14.9) approximately match the average gingiva parameters, as determined by Ho et al. [41] (L^* 57.5, b^* 22.2, b^* 14.4). The slight addition of TiO₂ matches the gingiva a^* parameter of Caucasian people, while the higher addition of TiO₂ makes PMMA brighter, as compared to the average gingiva color by Ho et al. [41]. As seen from the ΔE values (calculated as the difference between the average gingiva parameters [41] and these PMMA values), PMMA without TiO₂ has an ΔE higher than 3, a difference which is noticeable by eye.

According to the National Bureau of Standards, a color change is considered to be very low when ΔE is less than 1, clinically acceptable when ΔE is between 1 and 3, and clinically noticeable when ΔE exceeds 3 [55]. Chang et al. also considered the clinically acceptable ΔE^* value to be below 2.69, while all values exceeding this are considered clinically unacceptable [56].

Satisfactory aesthetics, including the appropriate color of the gingival part of the acrylate, is an important aspect of prosthetic rehabilitation [57,58]. Prosthesis wearers show parts of the anterior prosthetic segments during speech and laughter, which can look very unnatural if the color of the compensation is not adequate. Accordingly, the modification of PMMA by the addition of nanoparticles must not compromise the aesthetics of the restoration. Potential color changes resulting from the modification of conventional PMMA represent a very important segment of research. Acrylate-modified filler nanoparticles for denture base should improve the desired mechanical and biological properties without compromising on aesthetics [25,59,60].

In 2018, Aziz evaluated the color change after PMMA modification with 3wt% TiO₂ NP and measured that nanomodified samples were more flawed compared to pure PMMA.

The color change can occur because TiO₂ nanoparticles within the material absorb more light than the polymer matrix, increasing the inaccuracy of nanomodified samples compared to pure PMMA [59].

These results are related to the high atomic number of titanium compared to the low atomic number of acrylate chemical constituents. The results are consistent with the results of other studies using ZrO₂ nanoparticles, where the nanomodified material showed a statistically significant increase in light absorption, with light absorption increasing in proportion to the concentration of ZrO₂ nanoparticles [61].

Cierech et al. investigated the polymerization time and color change of PMMA for a denture base modified by the addition of 1% and 2% TiO₂ NPs. The obtained data reveal that the addition of both 1 wt% and 2 wt% causes a significant change in the color of PMMA, that became lighter. The color change between pure PMMA and PMMA/TiO₂ NP is significantly more noticeable than between 1 wt% PMMA/TiO₂ NP and 2 wt% PMMA/TiO₂ NP [62]. The reduced transparency of the formed material is caused by a high refractive index, which is characterized by TiO₂ NP [63].

Due to the significant color change, the authors suggest that the clinical application of PMMA/TiO₂ NPs would be limited to denture support, with new material located in an aesthetically invisible zone such as the imprint surface or polished parts of the prosthesis that have not been detected.

Denture base resins display varying color stability, and the color stability of polymethyl methacrylate denture base resin was greater as compared to polyamid [64].

Computer-aided design/computer-aided manufacturing (CAD/CAM) has become popular in restorative dentistry due to its efficiency in many ways. Regarding color stability, CAD/CAM-fabricated acrylics have achieved better stability as compared to conventional PMMA resins [65]. The reinforcement of PMMA with SiO₂ nanoparticles at 0.25 wt% increased the L* (brightness), decreased the a* (a change from red to green shades) and increased the b* value (a change from blue to yellow) [66].

4.6. Bacterial Adhesion Rate Measurement, SEM Micrographs

The pronounced bacterial adhesion was observed on surfaces with the lowest addition of TiO₂ nanoparticles. The bacterial adhesion was evaluated from a series of SEM micrographs (Figure 5). With an increase in TiO₂ concentration in the samples, the morphological change of bacteria takes place, which is observed by the SEM analysis. The results of single bacterial adhesion show a decrease in the value from 75% coverage in samples of pure PMMA to a value of 40% coverage in samples with 20% added nanoparticles. In the last measurements, an increased bacterial morphological change is observed and the coverage of samples with single *S. mutans* drops below 25%. Generally, the bacterial adhesion extent depends on the roughness, zeta potential and hydrophobicity, as well as on the bacteria surface properties [67]. In this study, the driving force for the bacterial adhesion is the increasing roughness and hydrophobicity.

In line with this study, Gad et al. reported that the addition of TiO₂ nanoparticles inhibits the adhesion of cariogenic bacteria to the acrylate surface, as well as shows strong antimicrobial activity in the planktonic phase and subsequent biofilm formation [25]. Similarly, Sodagar et al. also reported strong antimicrobial activity against cariogenic bacteria, including *L. acidophilus* and *S. mutans* in PMMA that was modified by the addition of TiO₂ and SiO₂ nanoparticles [68].

5. Conclusions

In this study, the impact of TiO₂ in PMMA on the antibacterial properties was examined. The aims of this study were to determine the effects of TiO₂ nanoparticles (in concentrations of 1%, 5%, 10% and 20%) on the uniaxial tensile strength of denture base PMMA, on the color change of the denture base PMMA and on the formation of *S. mutans* biofilm on the surface of the denture base PMMA. The following null hypotheses can be confirmed:

1. The addition of TiO₂ nanoparticles in concentrations of 1%, 5%, 10% and 20% affects the uniaxial tensile strength of denture base PMMA.
2. The addition of TiO₂ nanoparticles in concentrations of 1%, 5%, 10% and 20% affects the color change of the denture base PMMA.
3. The addition of TiO₂ nanoparticles in concentrations of 1%, 5%, 10% and 20% considerably affects the formation of *S. mutans* biofilm on the surface of the denture base PMMA; the single bacterial adhesion decays of 10% and 20% of added TiO₂ amounts to 58% and 60%, respectively.

The modification of denture base acrylic resin with TiO₂ NPs has an impact on bacterial adhesion. PMMA/TiO₂ NPS can be considered as a promising material for the fabrication of acrylic resin base dental materials. Further studies must test PMMA/TiO₂ enriched with other perspective materials in order to retain the antimicrobial properties and provide a color that will closely match that of the gingiva.

Author Contributions: Conceptualization: K.B.; Formal analysis: A.A., A.U., I.G., R.Š., A.S.Š. and R.V.; Investigation: A.A., F.R., R.Š. and A. Z.; Methodology: K.B., A.U. and A.Z.; Supervision: K.B.; Writing – original draft: K.B.; Writing – review & editing: A.A., A.S.Š., R.V., V.V., O.D. and A.Z. All authors have read and agreed to the published version of the manuscript.

Funding: K.B., V.V. and O.D. thank the bilateral project between Slovenia and BiH. K.B. thanks ARRS through the program Mechanisms of Health Maintenance for Financial Support, while A.S.Š. thanks ARRS for financial support through the program No. P2-0273: "Building structures and materials".

Institutional Review Board Statement: Not applicable.

Informed Consent Statement: Not applicable.

Data Availability Statement: All data that support the findings of this study are included within the article.

Acknowledgments: We acknowledge Aleš Traven and Jaka Vaupot for measuring tensile properties.

Conflicts of Interest: The authors declare no conflict of interest.

References

1. United Nations Department of Economic and Social Affairs Population Division. World Population Aging 2019. Available online: <https://www.un.org/en/development/desa/population/publications/pdf/ageing/WorldPopulationAgeing2019-Highlights.pdf> (accessed on 5 August 2022).
2. Kassebaum, N.J.; Bernabe, E.; Dahiya, M.; Bhandari, B.; Murray, C.J.; Marcenes, W. Global burden of severe tooth loss: A systematic review and meta-analysis. *J. Dent. Res.* **2014**, *93*, 20S–28S. [CrossRef] [PubMed]
3. Zafar, M.S. Prosthodontic Applications of Polymethyl Methacrylate (PMMA): An Update. *Polymers* **2020**, *12*, 2299. [CrossRef] [PubMed]
4. Kawaguchi, T.; Lassila, L.V.; Sasaki, H.; Takahashi, Y.; Vallittu, P.K. Effect of heat treatment of polymethyl methacrylate powder on mechanical properties of denture base resin. *J. Mech. Behav. Biomed. Mater.* **2014**, *39*, 73–78. [CrossRef] [PubMed]
5. Alp, G.; Johnston, W.M.; Yilmaz, B. Optical properties and surface roughness of prepolymerized poly(methyl methacrylate) denture base materials. *J. Prosthet. Dent.* **2019**, *121*, 347–352. [CrossRef] [PubMed]
6. Ali Sabri, B.; Satgunam, M.; Abreeza, N.; Abed, A.N. A review on enhancements of PMMA Denture Base Material with Different Nano-Fillers. *Cogent. Eng.* **2021**, *8*, 1875968. [CrossRef]
7. Adamovic, T.; Veselinovic, V.; Trtic, N.; Hadzi-Mihailovic, M.; Atlagić, S.G.; Balaban, M.; Yoshiyuki, H.; Hironori, S.; Ivanič, A.; Rudolf, R. Mechanical properties of new denture base material modified with gold nanoparticles. *J. Prosthodont. Res.* **2021**, *65*, 155–161. [CrossRef] [PubMed]
8. Ajaj-Alkordy, N.M.; Alsaadi, M.H. Elastic modulus and flexural strength comparisons of high-impact and traditional denture base acrylic resins. *Saudi Dent. J.* **2014**, *26*, 15–18. [CrossRef]
9. De Castro, D.T.; Valente, M.L.; Agnelli, J.A.; Lavato da Silva, C.H.; Watanabe, E.; Siqueira, R.L.; Alves, O.L.; Holtz, R.D.; dos Reis, A.C. In vitro study of the antibacterial properties and impact strength of dental acrylic resins modified with a nanomaterial. *J. Prosthet. Dent.* **2016**, *115*, 238–246. [CrossRef]
10. Gad, M.M.; Fouda, S.M.; Al-Harbi, F.A.; Năpănkangas, R.; Raustia, A. PMMA denture base material enhancement: A review of fiber, filler, and nanofiller addition. *Int. J. Nanomed.* **2017**, *12*, 3801–3812. [CrossRef]
11. Gad, M.M.; Al-Thobity, A.M.; Rahoma, A.; Abualsaud, R.; Al-Harbi, F.A.; Akhtar, S. Reinforcement of PMMA Denture Base Material with a Mixture of ZrO₂ Nanoparticles and Glass Fibers. *Int. J. Dent.* **2019**, *2019*, 2489393. [CrossRef]
12. Mahmood, W.S. The effect of incorporating carbon nanotubes on impact, transverse strength, hardness, and roughness to high impact denture base material. *J. Baghdad Coll. Dent.* **2015**, *27*, 96–99. [CrossRef]
13. Hameed, H.K.; Rahman, H.A. The effect of addition nano particle ZrO₂ on some properties of autoclave processed heat-cured acrylic denture base material. *J. Baghdad Coll. Dent.* **2015**, *27*, 32–39. [CrossRef]
14. Gad, M.M.; Abualsaud, R.; Rahoma, A.; Al-Thobity, A.M.; Al-Abidi, K.S.; Akhtar, S. Effect of zirconium oxide nanoparticles addition on the optical and tensile properties of polymethyl methacrylate denture base material. *Int. J. Nanomed.* **2018**, *9*, 283–292. [CrossRef]
15. Gendreau, L.; Loewy, Z.G. Epidemiology and etiology of denture stomatitis. *J. Prosthodont.* **2011**, *20*, 251–260. [CrossRef]
16. Charman, K.M.; Fernandez, P.; Loewy, Z.; Middleton, A.M. Attachment of *Streptococcus oralis* on acrylic substrates of varying roughness. *Lett. Appl. Microbiol.* **2009**, *48*, 472–477. [CrossRef] [PubMed]
17. Morgan, T.D.; Wilson, M. The effects of surface roughness and type of denture acrylic on biofilm formation by *Streptococcus oralis* in a constant depth film fermentor. *J. Appl. Microbiol.* **2001**, *91*, 47–53. [CrossRef] [PubMed]
18. Pinke, K.H.; Freitas, P.; Viera, N.A.; Honorio, H.M.; Porto, V.C.; Lara, V.S. Decreased production of proinflammatory cytokines by monocytes from individuals presenting Candida-associated denture stomatitis. *Cytokine* **2016**, *77*, 145–151. [CrossRef]
19. Lee, H.E.; Li, C.Y.; Chang, H.W.; Yang, Y.H.; Wu, J.H. Effects of different denture cleaning methods to remove *Candida albicans* from acrylic resin denture based material. *J. Dent. Sci.* **2011**, *6*, 216–220. [CrossRef]
20. Garcia, A.A.M.N.; Sugio, C.Y.C.; de Azevedo-Silva, L.J.; Gomes, A.C.G.; Batista, A.U.D.; Porto, V.C.; Soares, S.; Neppelenbroek, K.H. Nanoparticle-modified PMMA to prevent denture stomatitis: A systematic review. *Arch. Microbiol.* **2021**, *204*, 75. [CrossRef]
21. Giti, R.; Zomorodian, K.; Firouzmandi, M.; Zareshahrbadi, Z.; Rahmannasab, S. Antimicrobial Activity of Thermocycled Polymethyl Methacrylate Resin Reinforced with Titanium Dioxide and Copper Oxide Nanoparticles. *Int. J. Dent.* **2021**, *2021*, 6690806. [CrossRef]
22. Bacali, C.; Baldea, I.; Moldovan, M.; Carpa, R.; Olteanu, D.E.; Filip, G.A.; Nastase, V.; Lascu, L.; Badea, M.; Constantiniuc, M.; et al. Flexural strength, biocompatibility, and antimicrobial activity of a polymethyl methacrylate denture resin enhanced with graphene and silver nanoparticles. *Clin. Oral Investig.* **2020**, *24*, 2713–2725. [CrossRef] [PubMed]

23. Abdulrazzaq Naji, S.; Jafarzadeh Kashi, T.S.; Pourhajibagher, M.; Behroozibakhsh, M.; Masaeli, R.; Bahador, A. Evaluation of Antimicrobial Properties of Conventional Poly(Methyl Methacrylate) Denture Base Resin Materials Containing Hydrothermally Synthesised Anatase TiO₂ Nanotubes against Cariogenic Bacteria and *Candida albicans*. *Iran. J. Pharm. Res.* **2018**, *17*, 161–172. [[PubMed](#)]
24. Abualsaud, R.; Aleraky, D.M.; Akhtar, S.; Khan, S.Q.; Gad, M.M. Antifungal Activity of Denture Base Resin Containing Nanozirconia: In Vitro Assessment of *Candida albicans* Biofilm. *Sci. World J.* **2021**, *2021*, 5556413. [[CrossRef](#)]
25. Gad, M.M.; Abualsaud, R. Behavior of PMMA Denture Base Materials Containing Titanium Dioxide Nanoparticles: A Literature Review. *Int. J. Biomater.* **2019**, *2019*, 6190610. [[CrossRef](#)]
26. Alrahlah, A.; Fouad, H.; Hashem, M.; Niazy, A.A.; AlBadah, A. Titanium Oxide (TiO₂)/Polymethylmethacrylate (PMMA) Denture Base Nanocomposites: Mechanical, Viscoelastic and Antibacterial Behavior. *Materials* **2018**, *11*, 1096. [[CrossRef](#)] [[PubMed](#)]
27. Bangera, M.K.; Kotian, R.N.R. Effect of titanium dioxide nanoparticle reinforcement on flexural strength of denture base resin: A systematic review and meta-analysis. *Jpn. Dent. Sci. Rev.* **2020**, *56*, 68–76. [[CrossRef](#)] [[PubMed](#)]
28. Alwan, S.A.; Alameer, S.S. The effect of the addition of silanized nano titania fillers on some physical and mechanical properties of heat cured acrylic denture base materials. *J. Baghdad Coll. Dent.* **2015**, *27*, 86–91. [[CrossRef](#)]
29. Giti, R.; Firouzmandi, M.; Zare Khafri, N.; Ansarifard, E. Influence of different concentrations of titanium dioxide and copper oxide nanoparticles on water sorption and solubility of heat-cured PMMA denture base resin. *Clin. Exp. Dent. Res.* **2022**, *8*, 287–293. [[CrossRef](#)]
30. Chen, R.; Han, Z.; Huang, Z.; Karki, J.; Wang, C.; Zhu, B.; Zhang, X. Antibacterial activity, cytotoxicity and mechanical behavior of nano-enhanced denture base resin with different kinds of inorganic antibacterial agents. *Dent. Mater. J.* **2017**, *36*, 693–699. [[CrossRef](#)]
31. Totu, E.E.; Nechifor, A.C.; Nechifor, G.; Aboul-Enein, H.Y.; Cristache, C.M. Poly(methyl methacrylate) with TiO₂ nanoparticles inclusion for stereolithographic complete denture manufacturing—The future in dental care for elderly edentulous patients. *J. Dent.* **2017**, *59*, 68–77. [[CrossRef](#)]
32. Onwubu, S.C.; Vahed, A.; Singh, S.; Kanny, K.M. Reducing the surface roughness of dental acrylic resins by using an eggshell abrasive material. *J. Prosthet. Dent.* **2017**, *117*, 310–314. [[CrossRef](#)] [[PubMed](#)]
33. Pereira-Cenci, T.; Pereira, T.; Cury, A.A.; Cenci, M.S.; Rodrigues-Garcia, R.C.M. In vitro *Candida* colonization on acrylic resins and denture liners: Influence of surface free energy, roughness, saliva, and adhering bacteria. *Int. J. Prosthodont.* **2007**, *20*, 308–310. [[PubMed](#)]
34. Dos Santos, R.L.O.; Sarra, G.; Lincopan, N.; Petri, D.F.S.; Aliaga, J.; Marques, M.M.; Dias, R.B.; Coto, N.P.; Sugaya, N.N.; Paula, C.R. Preparation, antimicrobial properties, and cytotoxicity of acrylic resins containing poly(diallyldimethylammonium chloride). *Int. J. Prosthodont.* **2020**, *26*, 1–7. [[CrossRef](#)] [[PubMed](#)]
35. Cheng, Y.; Sakai, T.; Moroi, R.; Moroi, R.; Nakagawa, M.; Sakai, H.; Ogata, T.; Terada, Y. Self-cleaning ability of a photocatalyst-containing denture base material. *Dent. Mater. J.* **2008**, *27*, 179–186. [[CrossRef](#)] [[PubMed](#)]
36. Høiby, N.; Ciofu, O.; Johansen, H.K.; Song, Z.J.; Moser, C.; Jensen, P.Ø.; Molin, S.; Givskov, M.; Tolker-Nielsen, T.; Bjarnsholt, T. The clinical impact of bacterial biofilms. *Int. J. Oral Sci.* **2011**, *3*, 55–65. [[CrossRef](#)] [[PubMed](#)]
37. Hengzhuang, W.; Wu, H.; Ciofu, O.; Song, Z.J.; Høiby, N. In vivo pharmacokinetics/pharmacodynamics of colistin and imipenem in *Pseudomonas aeruginosa* biofilm infection. *Antimicrob. Agents Chemother.* **2012**, *56*, 2683–2690. [[CrossRef](#)]
38. Høiby, N.; Bjarnsholt, T.; Givskov, M.; Molin, S.; Ciofu, O. Antibiotic resistance of bacterial biofilms. *Int. J. Antimicrob. Agents.* **2010**, *35*, 322–332. [[CrossRef](#)]
39. Besinis, A.; Hadi, S.D.; Le, H.R.; Tredwin, C.; Handy, R.D. Antibacterial activity and biofilm inhibition by sur-709 face modified titanium alloy medical implants following application of silver, titanium dioxide and hydroxyapatite nanocoatings. *Nanotoxicology* **2017**, *11*, 327–338. [[CrossRef](#)]
40. Pelgrift, R.Y.; Friedman, A.J. Nanotechnology as a therapeutic tool to combat microbial resistance. *Adv. Drug Deliv. Rev.* **2013**, *65*, 1803–1815. [[CrossRef](#)]
41. Ho, D.K.; Ghinea, R.; Herrera, L.J.; Angelov, N.; Paravina, R.D.J.S.R. Color range and color distribution of healthy human gingiva: A prospective clinical study. *Sci. Rep.* **2015**, *5*, 1–7. [[CrossRef](#)]
42. Arunachalam, A.; Dhanapandian, S.; Manoharan, C.; Sivakumar, G. Physical properties of Zn doped TiO₂ thin films with spray pyrolysis technique and its effects in antibacterial activity. *Spectrochim. Acta Part A Mol. Biomol. Spectrosc.* **2015**, *138*, 105–112. [[CrossRef](#)] [[PubMed](#)]
43. Chatterjee, A. Properties improvement of PMMA using nano TiO₂. *J. Appl. Polym. Sci.* **2010**, *118*, 2890–2897. [[CrossRef](#)]
44. Shirkavand, S.; Moslehifard, E. Effect of TiO₂ Nanoparticles on Tensile Strength of Dental Acrylic Resins. *J. Dent. Res. Dent. Clin. Dent. Prospect.* **2014**, *8*, 197–203.
45. Sun, J.; Forster, A.M.; Johnson, P.M.; Eidelman, N.; Quinn, G.; Schumacher, G. Improving performance of dental resins by adding titanium dioxide nanoparticles. *Dent. Mater.* **2011**, *27*, 972–982. [[CrossRef](#)] [[PubMed](#)]
46. Moslehifard, E.; Robati Anaraki, M.; Shirkavand, S. Effect of adding TiO₂ nanoparticles on the SEM morphology and mechanical properties of conventional heat-cured acrylic resin. *J. Dent. Res. Dent. Clin. Dent. Prospect.* **2019**, *13*, 234–240. [[CrossRef](#)] [[PubMed](#)]
47. Mosalman, S.; Rashahmadi, S.; Hasanzadeh, R. The effect of TiO₂ nanoparticles on mechanical properties of poly methyl methacrylate nanocomposites. *Int. J. Eng. Trans. B Appl.* **2017**, *30*, 807–813.

48. Ghahremani, L.; Shirkavand, S.; Akbari, F.; Sabzikari, N. Tensile strength and impact strength of color modified acrylic resin reinforced with titanium dioxide nanoparticles. *J. Clin. Exp. Dent.* **2017**, *9*, 661–665. [[CrossRef](#)]
49. Ahmed, M.A.; El-Shennawy, M. Effect of titanium dioxide nano particles incorporation on mechanical and physical properties on two different types of acrylic resin denture base. *World J. Nano Sci. Eng.* **2016**, *6*, 111. [[CrossRef](#)]
50. Bohinc, K.; Dražič, G.; Fink, R.; Oder, M.; Jevšnik, M.; Nipič, D.; Godič Torkar, K.; Raspor, P. Available surface dictates microbial adhesion capacity. *Int. J. Adhes. Adhes.* **2014**, *50*, 265–272. [[CrossRef](#)]
51. Bohinc, K.; Dražič, G.; Abram, A.; Jevšnik, M.; Jeršek, B.; Nipič, D.; Kurinčič, M.; Raspor, P. Metal surface characteristics dictate bacterial adhesion capacity. *Int. J. Adhes. Adhes.* **2016**, *68*, 39–46. [[CrossRef](#)]
52. Janovak, L.; Deak, A.; Tallosy, S.P.; Sebok, D.; Csapo, E.; Bohinc, K.; Abram, A.; Palinko, A.; Dekany, I. Hydroxyapatite-enhanced structural, photocatalytic and antibacterial properties of photoreactive TiO₂/HAp/polyacrylate hybrid thin films. *Surf. Coat. Technol.* **2017**, *326*, 316–326. [[CrossRef](#)]
53. Hengzhuang, W.; Wu, H.; Ciofu, O.; Song, Z.; Høiby, N. Pharmacokinetics/pharmacodynamics of colistin and imipenem on mucoid and nonmucoid *Pseudomonas aeruginosa* biofilms. *Antimicrob. Agents Chemother.* **2011**, *55*, 4469–4474. [[CrossRef](#)] [[PubMed](#)]
54. Hashem, M.; Al Rez, M.F.; Fouad, H. Influence of titanium oxide nanoparticles on the physical and thermomechanical behavior of poly methyl methacrylate (pmma): A denture base resin. *Sci. Adv. Mater.* **2017**, *9*, 938–944. [[CrossRef](#)]
55. Andreotti, A.M. Influence of nanoparticles on color stability, microhardness, and flexural strength of acrylic resins specific for ocular prosthesis. *Int. J. Nanomed.* **2014**, *9*, 5779–5787.
56. Chang, J.; Da Silva, J.D.; Sakai, M.; Kristiansen, J.; Ishikawa Nagai, S. The optical effect of composite luting cement on all ceramic crowns. *J. Dent.* **2009**, *37*, 937–943. [[CrossRef](#)]
57. Chu, S.J.; Devigus, A.; Mieleszko, A.J. *Fundamentals of Color: Shade Matching and Communication in Esthetic Dentistry*; Quintessence Publishing Co., Inc.: Batavia, IL, USA, 2004.
58. Gómez-Polo, C.; Montero, J.; Gómez-Polo, M.; Martín Casado, A.M. Clinical study on natural gingival color. *Odontology* **2019**, *107*, 80–89. [[CrossRef](#)]
59. Aziz, H.K. TiO-Nanofillers Effects on Some Properties of Highly-Impact Resin Using Different Processing Techniques. *Open Dent. J.* **2018**, *12*, 202–212. [[CrossRef](#)]
60. Acosta-Torres, L.S.; López-Marín, L.M.; Nunez-Anita, R.E.; Hernández-Padrón, G.; Castaño, V.M. Biocompatible Metal Oxide Nanoparticles: Nanotechnology Improvement of Conventional Prosthetic Acrylic Resins. *J. Nanomater.* **2011**, *2011*, 941561. [[CrossRef](#)]
61. Ihab, N.S.; Hassanen, K.A.; Ali, N.A. Assessment of zirconium oxide nano-fillers incorporation and silanation on impact, tensile strength and color alteration of heat polymerized acrylic resin. *J. Baghdad Coll. Dent.* **2012**, *24*, 36–42.
62. Cierech, M.; Szerszeń, M.; Wojnarowicz, J.; Łojkowski, W.; Kostrzewa-Janicka, J.; Mierzwińska-Nastalska, E. Preparation and Characterisation of Poly(methyl methacrylate)-Titanium Dioxide Nanocomposites for Denture Bases. *Polymers* **2020**, *12*, 2655. [[CrossRef](#)]
63. Manerat, C.; Hayata, Y. Antifungal activity of TiO₂ photocatalysis against *Penicillium expansum* in vitro and in fruit tests. *Int. J. Food Microbiol.* **2006**, *107*, 99–103. [[CrossRef](#)]
64. Sagsoz, N.P.; Yanikoglu, N.; Ulu, H.; Bayındır, F. Color changes of polyamid and polymethyl methacrylate denture base materials. *Open J. Stomatol.* **2014**, *4*, 489. [[CrossRef](#)]
65. Dimitrova, M.; Corsalini, M.; Kazakova, R.; Vlahova, A.; Barile, G.; Dell’Olio, F.; Tomova, Z.; Kazakov, S.; Capodiferro, S. Color Stability Determination of CAD/CAM Milled and 3D Printed Acrylic Resins for Denture Bases: A Narrative Review. *J. Compos. Sci.* **2022**, *6*, 201. [[CrossRef](#)]
66. Kotanidis, A.; Kontonasaki, E.; Koidis, P. Color alterations of a PMMA resin for fixed interim prostheses reinforced with silica nanoparticles. *J. Adv. Prosthodont.* **2019**, *11*, 193–201. [[CrossRef](#)] [[PubMed](#)]
67. Filipović, U.; Dahmane, R.G.; Ghannouchi, S.; Zore, A.; Bohinc, K. Bacterial adhesion on orthopedic implants. *Adv. Colloid Interface Sci.* **2020**, *283*, 102228. [[CrossRef](#)]
68. Sodagar, A.; Khalil, S.; Kassaee, M.Z.; Shahroudi, A.S.; Pourakbari, B.; Bahador, A. Antimicrobial properties of poly(methyl methacrylate) acrylic resins incorporated with silicon dioxide and titanium dioxide nanoparticles on cariogenic bacteria. *J. Orthod. Sci.* **2016**, *5*, 7–13.